Impedance and Beam Stability in the SLC

K. Bane

Damping Rings

See:

L. Rivkin, et al - 1988 EPAC P. Krejcik, et al - 1993 Part. Acc. Conf. K. Bane, et al - 1995 Part. Acc. Conf.	Measurements
K. Bane - 1988 EPAC K. Bane + C.-K. Ng - 1993 Part. Acc. Conf.	Impedance Calculations
K. Bane + R. Ruth - 1989 Part. Acc. Conf. K. Bane + K. Oide - 1993 Part. Acc. Conf. K. Bane + K. Oide - 1995 Part. Acc. Conf.	Instability Calculations
K. Oide - KEK-Preprint-94-138, Nov 1994 A. Chao, et al - 1995 Part. Acc. Conf. B. Chen - 1995 Part. Acc. Conf.	Theory of Weak Instability in Resistive Machines

R. Holtzapple - Thesis - Bunch length measurements

B. Podobedov - Thesis - Saw tooth measurements

Longitudinal Wakefield Effects

- potential well distortion → bunch lengthening
- microwave instability
  - increased energy spread
    ↳ bunch lengthening
  - transient phenomena - eg "saw-tooth"
- heating of components

Effects on Downstream Linear Collider

- longer bunch will have stronger wakefield effects in linac
- more initial energy spread will lead to more chromatic emittance growth
- transient behavior will tend to amplify in linac

Approaches to Impedance

Want:

(1) a "Green function" wakefield

(2) to analyze which objects are important

For most objects use time domain, Maxwell Eq solver, like MAFIA

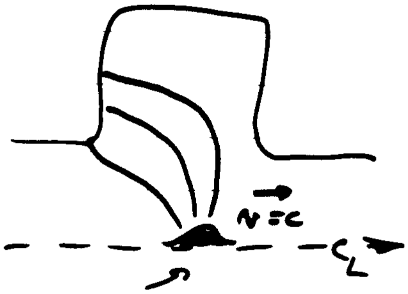

Green function bunch, length σ_ℓ

to model instability need ~ an oscillation over the bunch

$$\Rightarrow \sigma_\ell \lesssim \frac{\sigma_z}{5}$$

Note:

- for accuracy MAFIA requires mesh size $\Delta \lesssim \frac{\sigma_\ell}{5}$

  $\therefore$ for 3D objects (eg septum) may be impossible to get an accurate Green function

  $\Rightarrow$ may need to use very simple models, or ignore

- for a few simple, small objects (e.g. a small hole in beam tube wall) analytic formulas exist

  see eg reports by S. Kurennoy

For a careful ring impedance calculation (which doesn't completely satisfy all these problems) see work on Daphne ring

S. Bartalucci, et al, NIM A-337 (1994)

Types of Impedances [Numerical results for Gaussian bunch with $\sigma_z = 6\,mm$]

An Inductive Example: $V_{ind} \sim -L \frac{dI}{dt}$

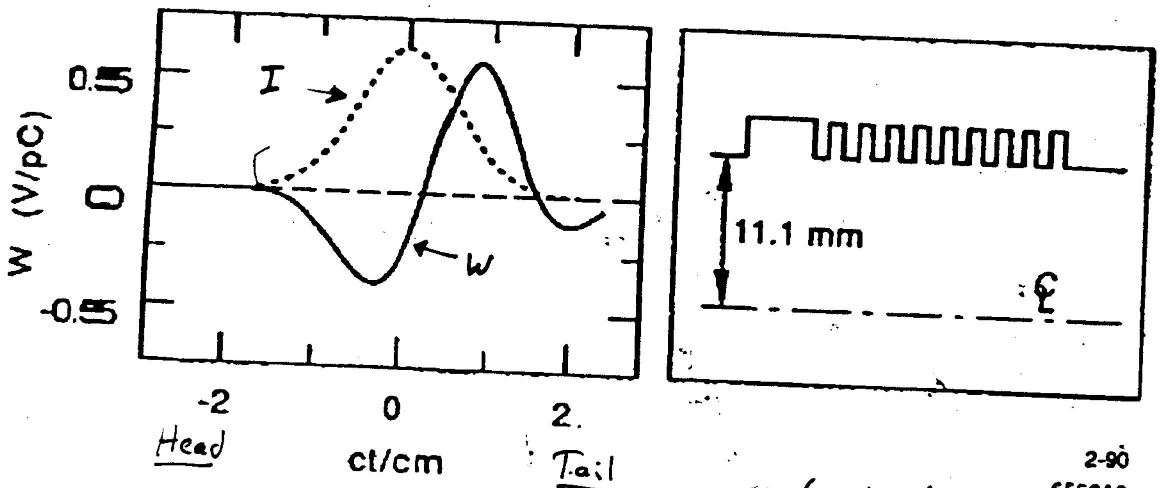

SLC (unshielded) bellows

Note: $V_{ind} = eNW$

A Capacitive Example: $V_{ind} \sim -\frac{1}{C} \int I dt$

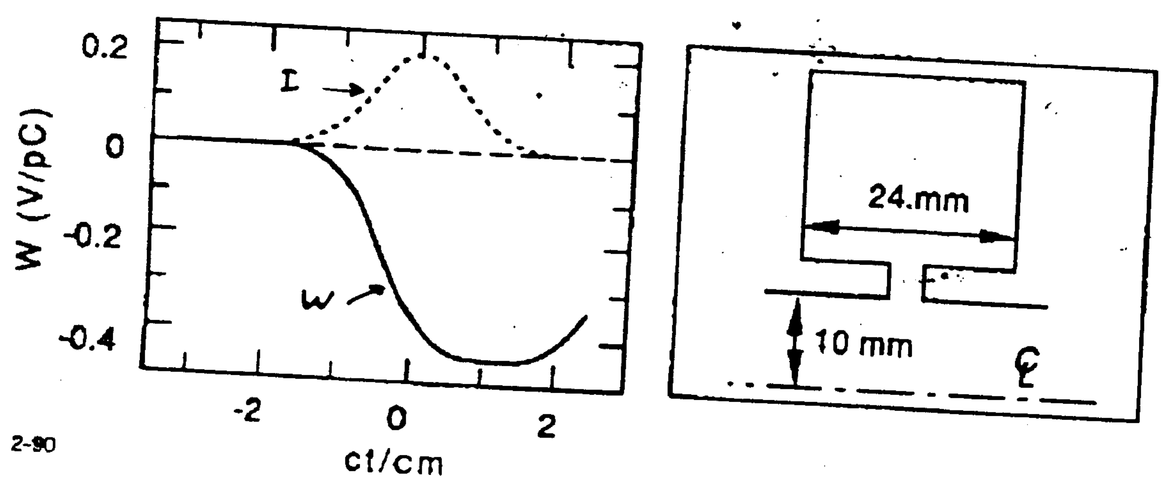

Model cavity 6562A5

A Resistive Example: $V_{ind} \sim -RI$

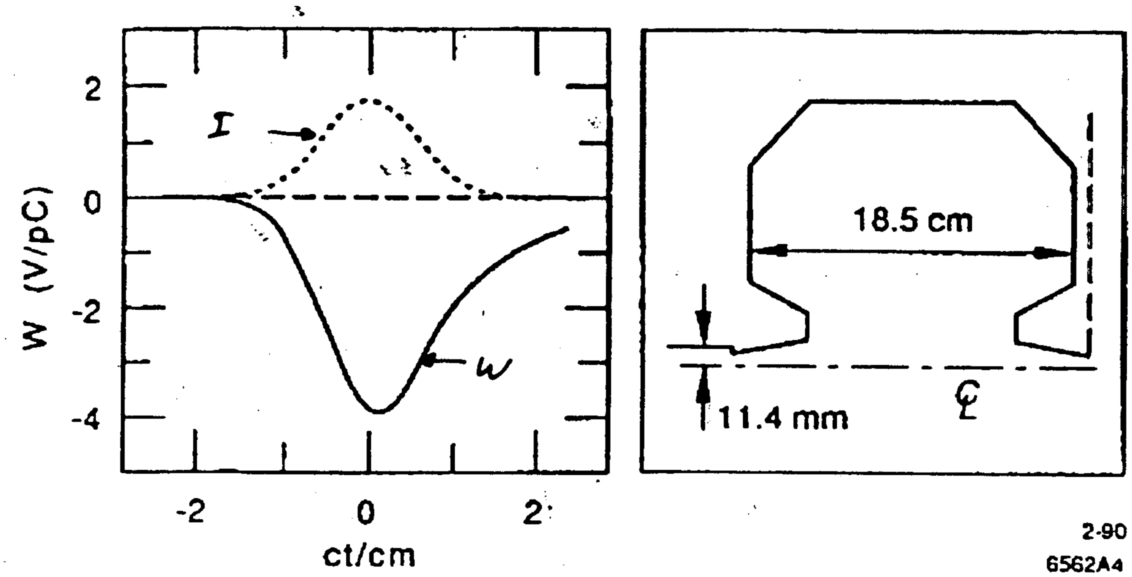

One cell of SLC rf cavity

SLC Damping Ring

History	
Old, old ring	original
Old ring	bellows shielded
Current ring	new vacuum chamber

Old Ring

Layout

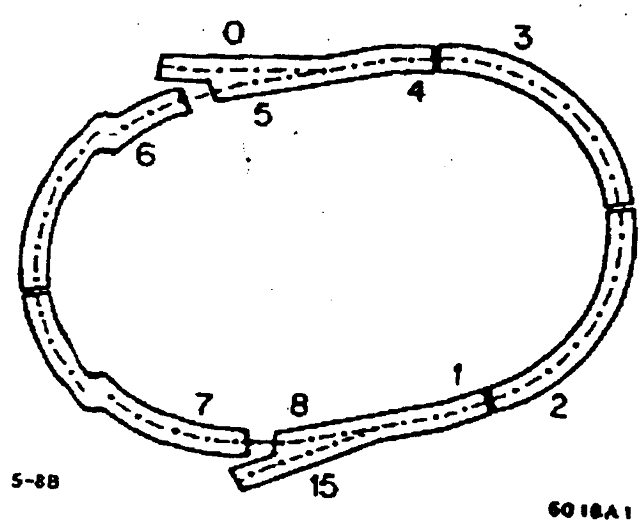

Circumference = 35m

Fig. 6. Three girders of the SLC north damping ring.

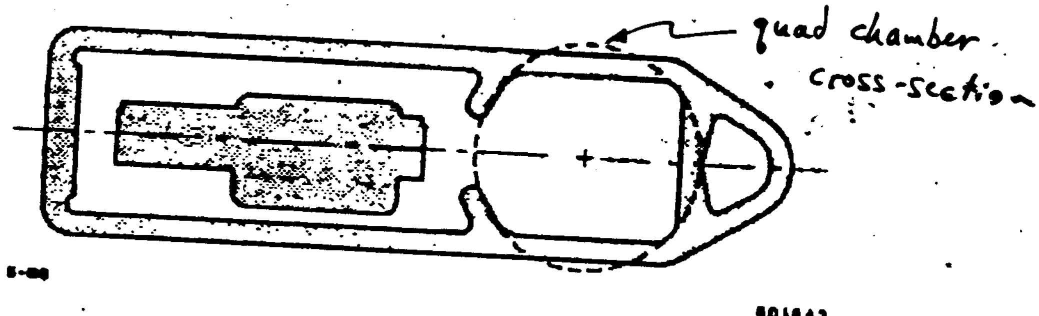

Fig. 7. The cross-section of the bend chamber. The dashed circle shows the size of a quad chamber.

Bend chamber cross-section

<u>Quad segments in old vacuum chamber</u>

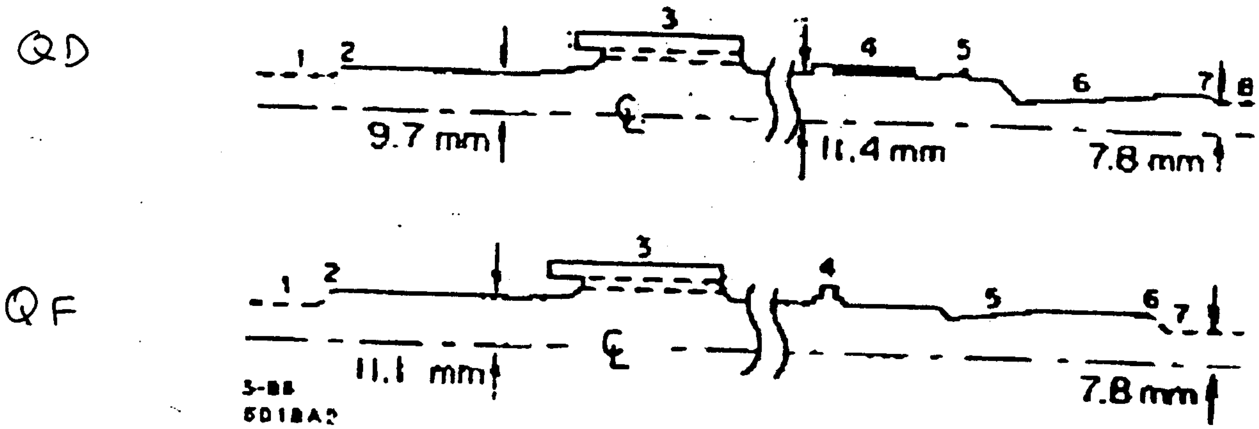

Fig. 8. The vertical profile of a QD segment (top) and a QF segmen (bottom). The noncylindrically symmetric portions are drawn with dashes

Table 1. The inductive vacuum chamber elements.

Single Element Inductance		Contribution in Ring		
Type	L/(nH)	Factor	Number	L/(nH)
QD bellows	0.62	1.0	20	12.5 later shielded
QD & QF masks	0.47	1.0	20	9.5
QD & QF trans.	0.52	0.9	20	9.3
Ion pump slots	1.32	0.1	40	5.3
Kicker bellows	2.03	1.0	2	4.1
Flex joint	0.18	1.0	20	3.6
1″ BPM trans.	0.10	0.8	40	3.3
Other				2.4
		Total		50.0

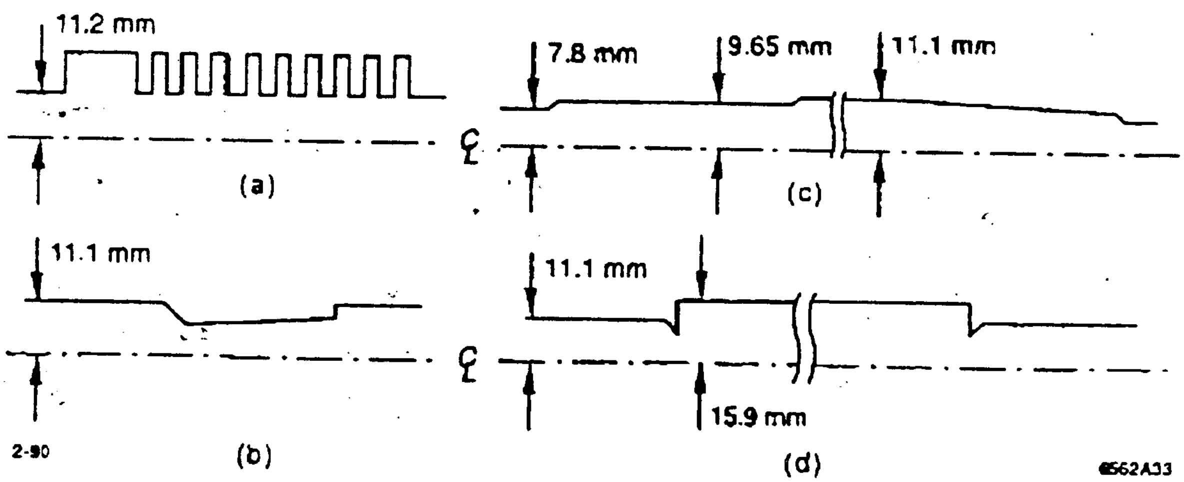

Fig. 9. The geometries used to calculate ℓ for: (a) the QD bellows, (b) the QD mask, (c) the QD transition, and (d) the pump slots.

Resistive Objects

RF cavities - $R = 411\,\Omega$

BPM cavities - $R = 227\,\Omega$

Total Calculated Wakefield for $\sigma_z = 1$ mm Bunch

Used as Green function

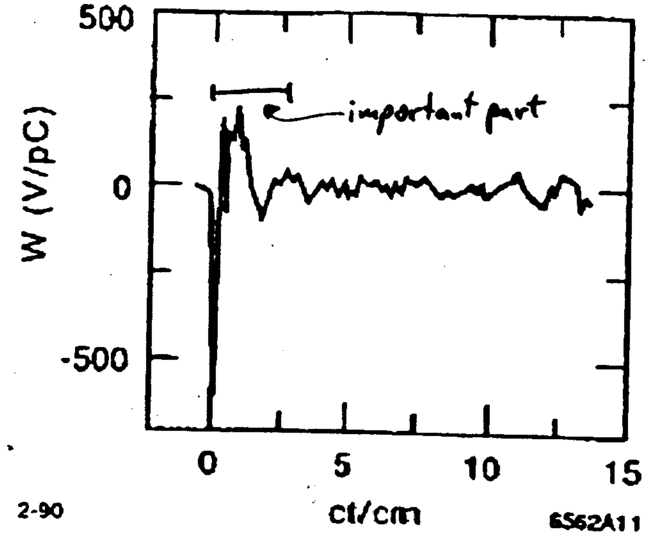

Fig. 10. The longitudinal wakefield of a 1 mm Gaussian bunch in the SLC damping ring.

Fourier Transform: Impedance

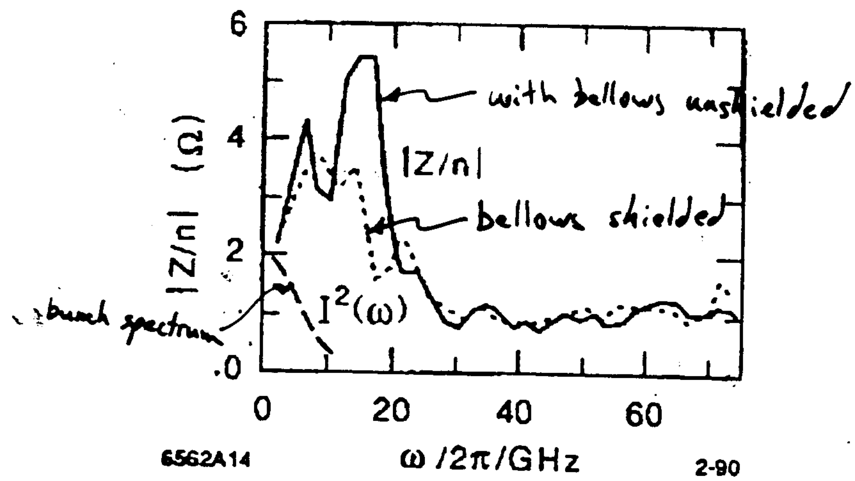

Fig. 13. The impedance $|Z/n|$ of the damping ring. The dots give what remains when the QD bellows (with their antechambers) are perfectly shielded. The power spectrum of a 6 mm Gaussian bunch is also shown.

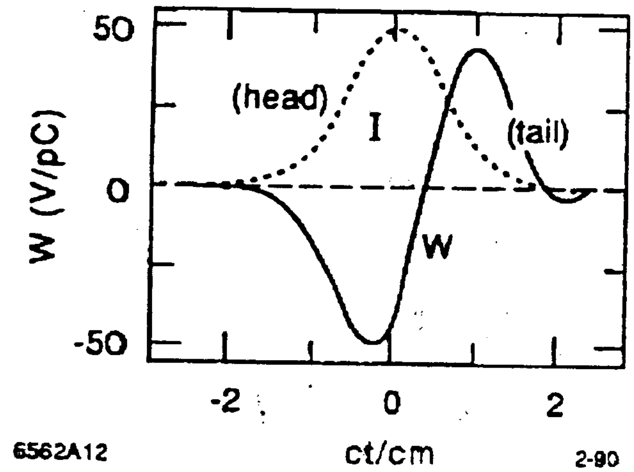

Wake of 6 mm Gaussian bunch

Note inductive character

Fig. 11. The longitudinal wakefield of a 6 mm Gaussian bunch in the SLC damping ring. The current distribution is also shown.

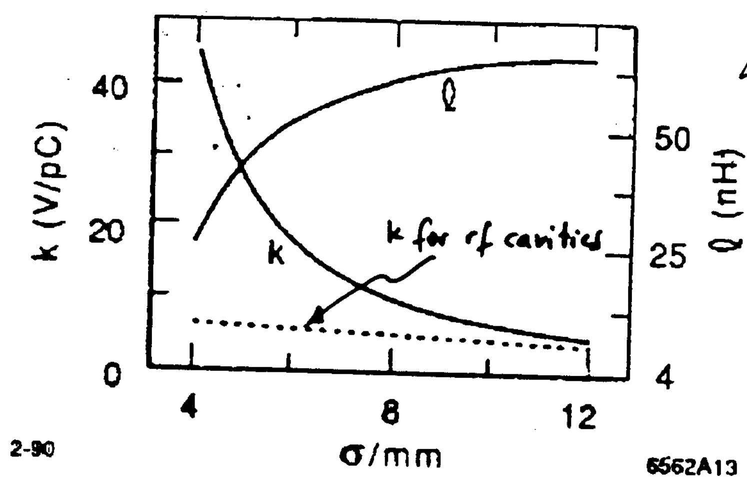

Loss factor k, Effective Inductance ℓ as function of σ_z

Fig. 12. The loss factor k and the effective inductance ℓ of the damping ring as function of bunch length. The dotted curve gives the loss contribution of the rf cavities alone.

Potential Well Distortion

Below threshold the steady-state distribution is given by the Haïssinki Equation:

$$I(t) = K \exp\left(\frac{-t^2}{2\sigma_0^2} + \frac{1}{\dot{V}_{rf}\,\sigma_0^2}\int_0^\infty S(t')\,I(t-t')\,dt'\right)$$

with $S(t) = \int_0^t W_p(t')\,dt'$;

σ_0 - nominal bunch length
$\dot{V}_{rf}$ - slope of rf voltage
K - normalizing constant

- Note: $\dot{V}_{rf}\langle t\rangle = eNk_{loss}$

Boussard Criterion of threshold to strong instability

$$\frac{e\hat{I}\,|Z(n)/n|}{2\pi\alpha E\sigma_\epsilon^2} \lesssim 1$$

$\hat{I}$ peak current
α momentum compaction
E energy
σ_ϵ energy spread
n ω/ω_0, ω_0 revolution frequency

Note - independent of radiation damping time otential Well Distortion for Some Impedances

Inductive

Note: no losses

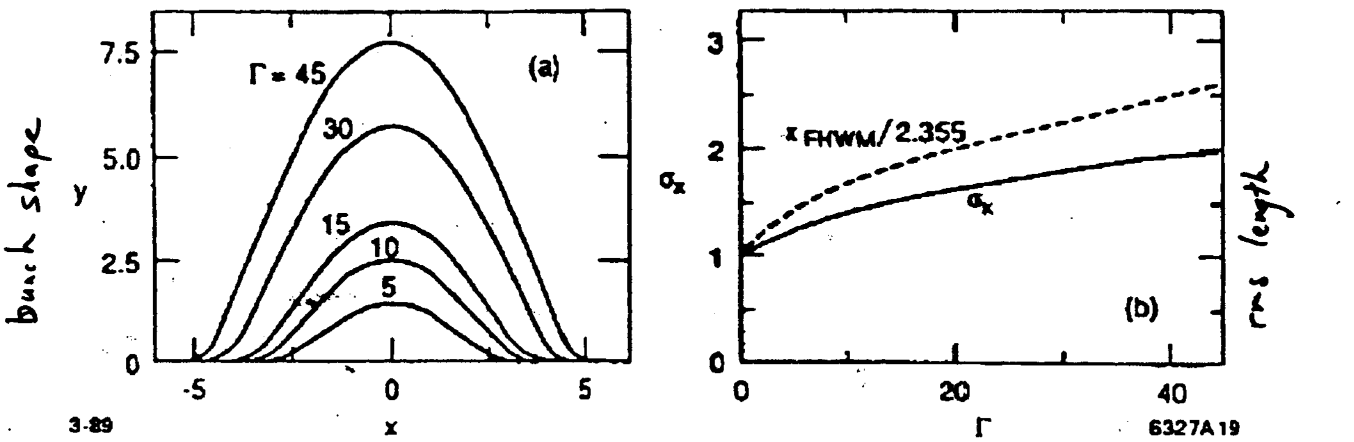

Fig. 20. An inductive impedance: (a) the bunch shape for several values of bunch population and (b) the bunch length variation as a function of current.

incoherent tune distribution

Note: very wide

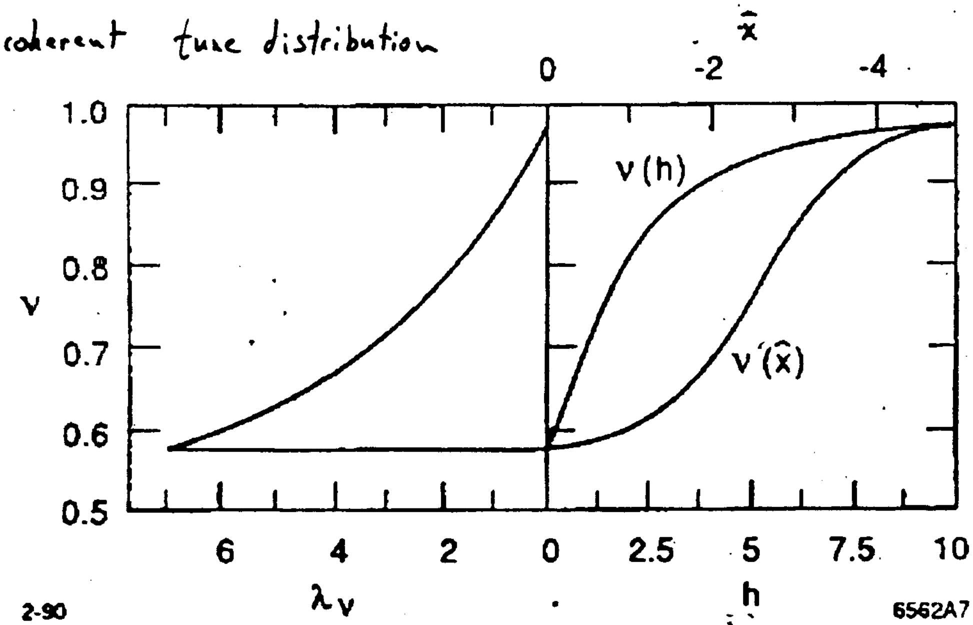

Fig. 21. (a) The tune distribution and (b) the dependence of tune on $\hat{x}$ and h when $\Gamma = 7.5$ for an inductive impedance.

Equivalent to ~ 1.5×10^{10} in SLC damping ring

Capacitive Model

Note: - bunch shortening
- $\langle x \rangle = -\Gamma/2$

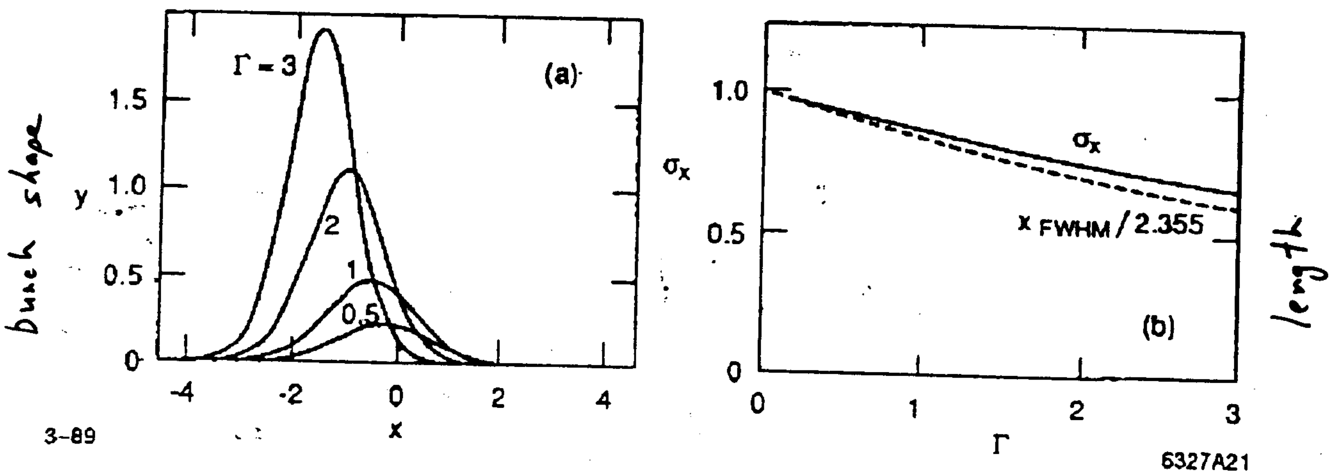

Fig. 26. (a) The bunch shape for various currents and (b) bunch shortening as a function of current, for a capacitive impedance.

Resistive Model

Note: little bunch lengthening

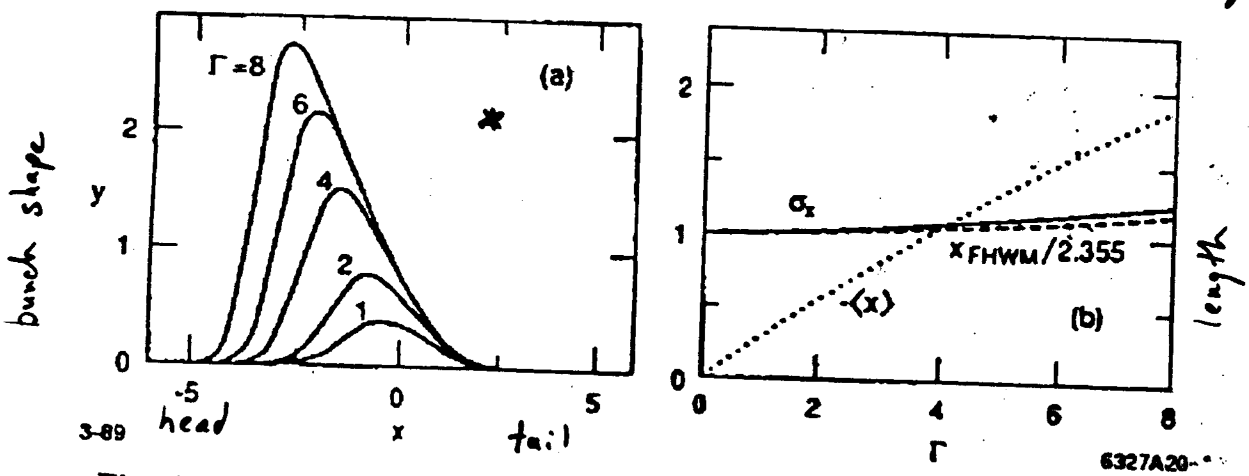

Fig. 23. A resistive impedance: (a) the bunch shape for several values of total charge and (b) the change of bunch length and centroid position (dots) with current. *[for analytic solution see, A. Ruggiero, et al, IEEE Trans. Nucl. Sci. NS-24 1977]

incoherent tune distribution

Note: Very little tune spread

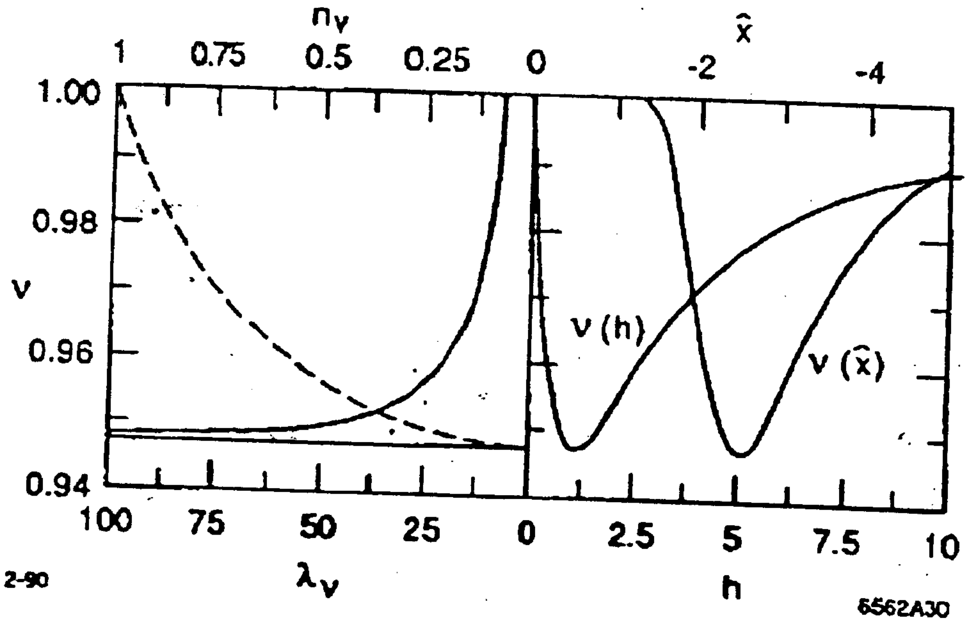

Fig. 24. (a) The tune distribution and its integral (dashes) and (b) the dependence of tune on $\hat{x}$ and h when $\Gamma = 3.4$ for a resistive impedance.

Old SLC Measurements

ooo measurements

— calculations using Green function

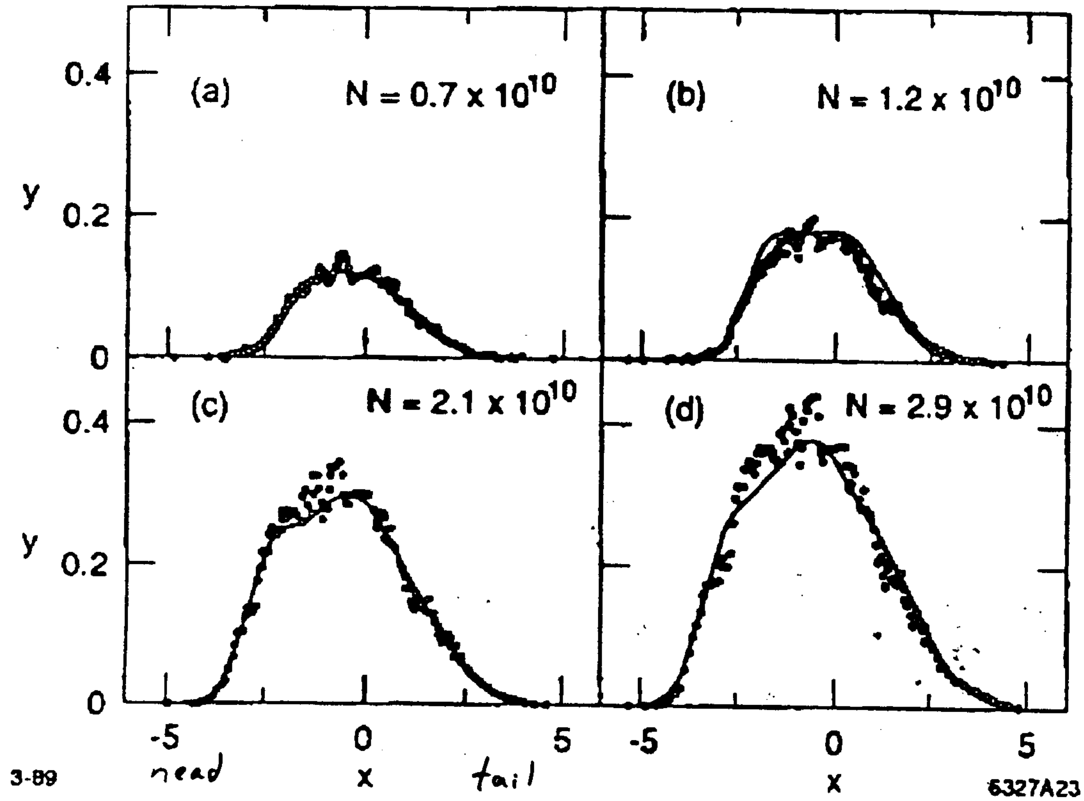

Fig. 28. The calculated damping ring bunch shapes for several current values, when V_{rf} = 0.8 MV. Superimposed on the curves are the measurement results.

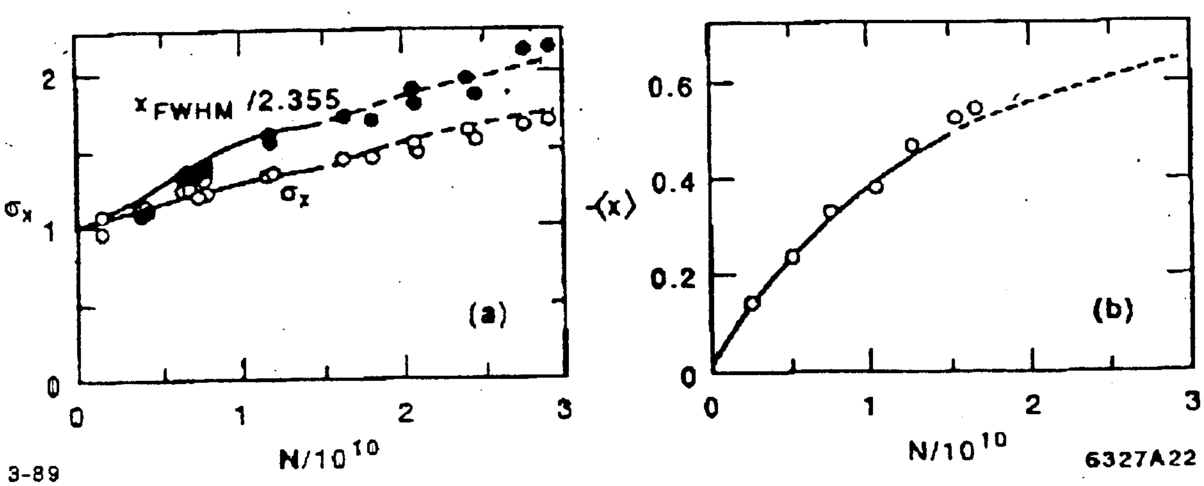

Fig. 27. (a) Bunch lengthening and (b) the centroid shift calculated for the SLC damping rings at V_{rf} = 0.8 MV. The symbols indicate the measurement results.

Tracking

See eg. R. Siemann, NIM 203, 57 (1982).

follow (ϵ_i, z_i) for 100,000's of macro-particles

$$\Delta\epsilon_i = -\frac{2T_0}{\tau_d}\epsilon_i + 2\sigma_{\epsilon 0}\sqrt{\frac{T_0}{\tau_d}}\, r_i + V_{rf}' z_i + V_{ind}(z_i)$$

$$\Delta z_i = \frac{\alpha c T_0}{E_0}(\epsilon_i + \Delta\epsilon_i)$$

with $V_{ind}(z) = -eN\int_{-\infty}^{z} W(z-z')\lambda_z(z')\,dz'$

- T_0 revolution period
- τ_d damping time
- α momentum compaction
- E_0 energy
- r_i : random number $\langle r_i \rangle = 0$, $\langle r_i^2 \rangle = 1$
- $\sigma_{\epsilon 0}$ nominal energy spread

Vlasov Eqn Solution

Computer program that solves perturbatively the time independent Vlasov Eqn., including the effects of potential well distortion, looking for unstable modes

K. Oide, K. Yokoya, KEK preprint 90-10, 1990.

Simulation above threshold

K. Bane, K. Oide, 1993. PAC.

projection of phase space

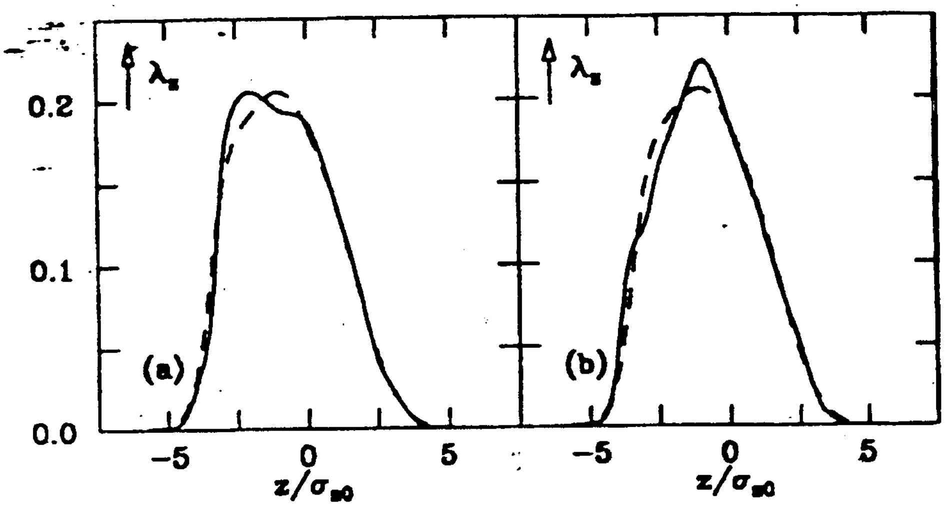

Fig. 5. A snapshot of the beam, at two phases 180° apart, when $N = 3.5 \times 10^{10}$.

longitudinal phase space (with average subtracted)

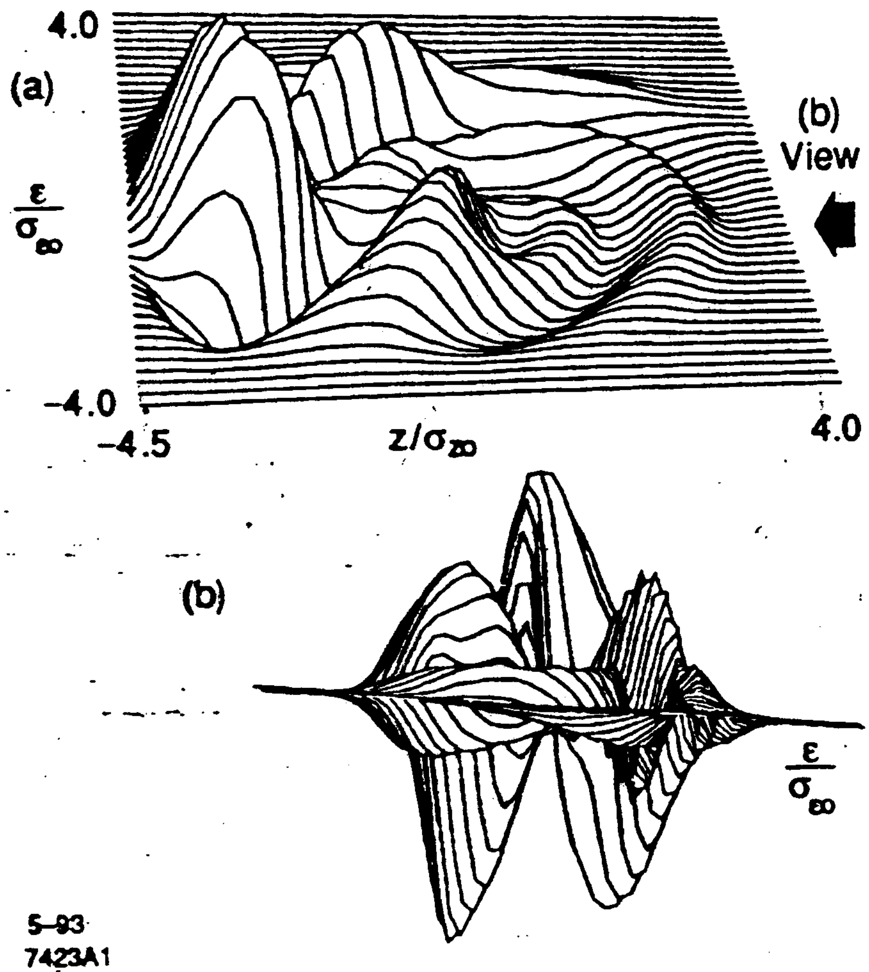

Fig. 6. The shape of the unstable mode from two views at $N = 3.5 \times 10^{10}$.

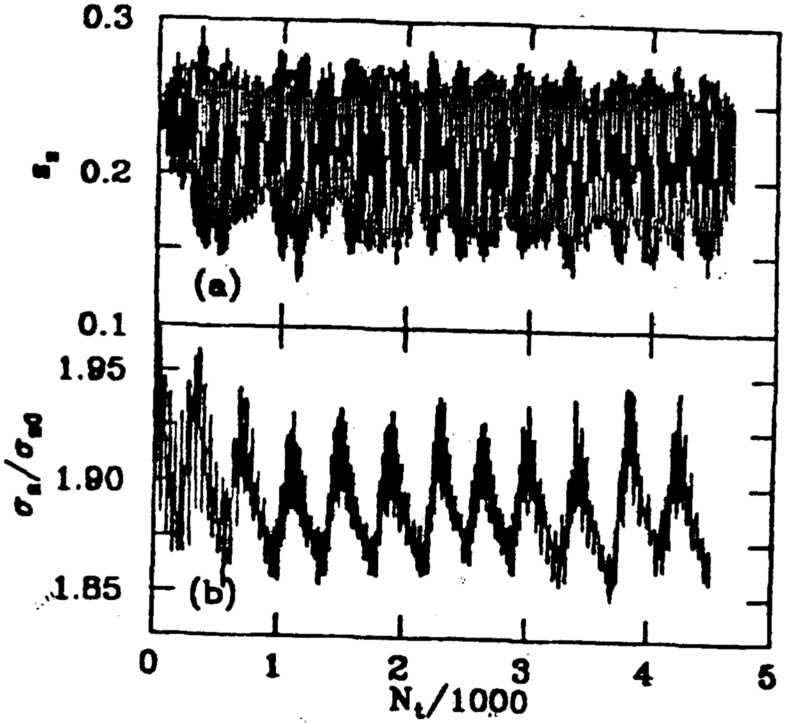

skew moment at 3.5×10^{10}

rms at 5.0×10^{10}

Fig. 3. The turn-by-turn skew when $N = 3.5 \times 10^{10}$ (a), and the rms when $N = 5.0 \times 10^{10}$ (b).

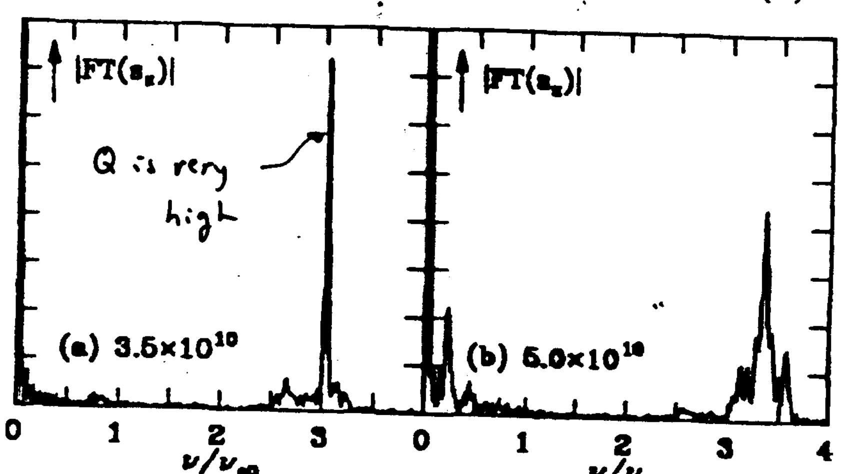

Fourier transforms

Fig. 4. The absolute value of the Fourier transform of the skew signal for two currents.

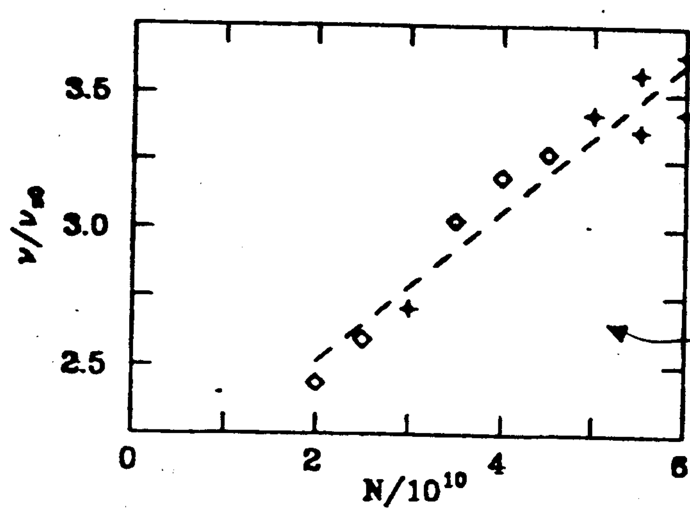

Coherent tune as function of current

agrees rather well with measurements

Fig. 7. The positions of the major peaks in the Fourier transform of the skew signal *vs* N.

9/22/1993

Frequency and Amplitude Dependence of Excited Modes as a Function of Beam Current with V_c=960 kV

Measured

M. Minty

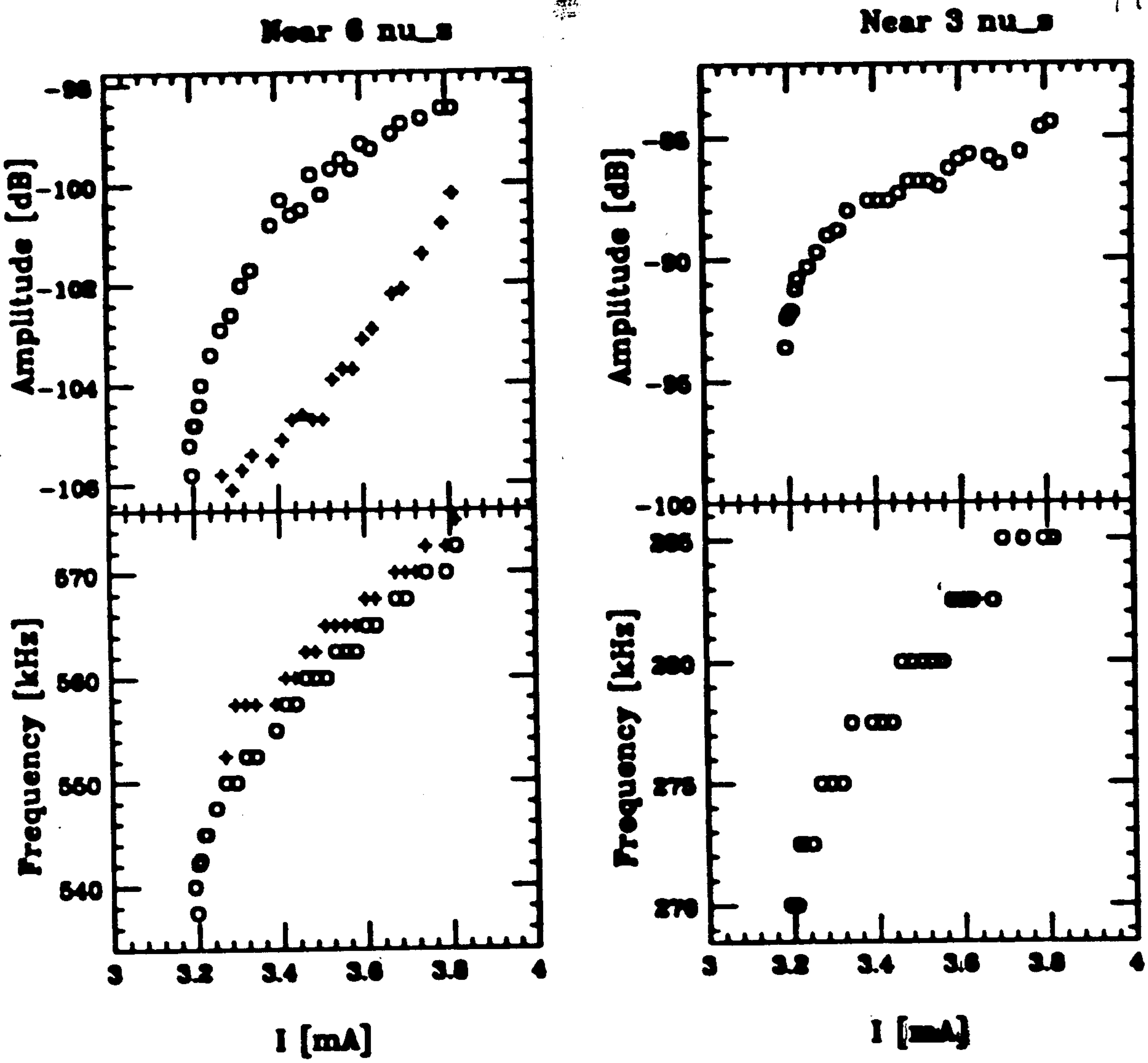

~~present~~ ring wake

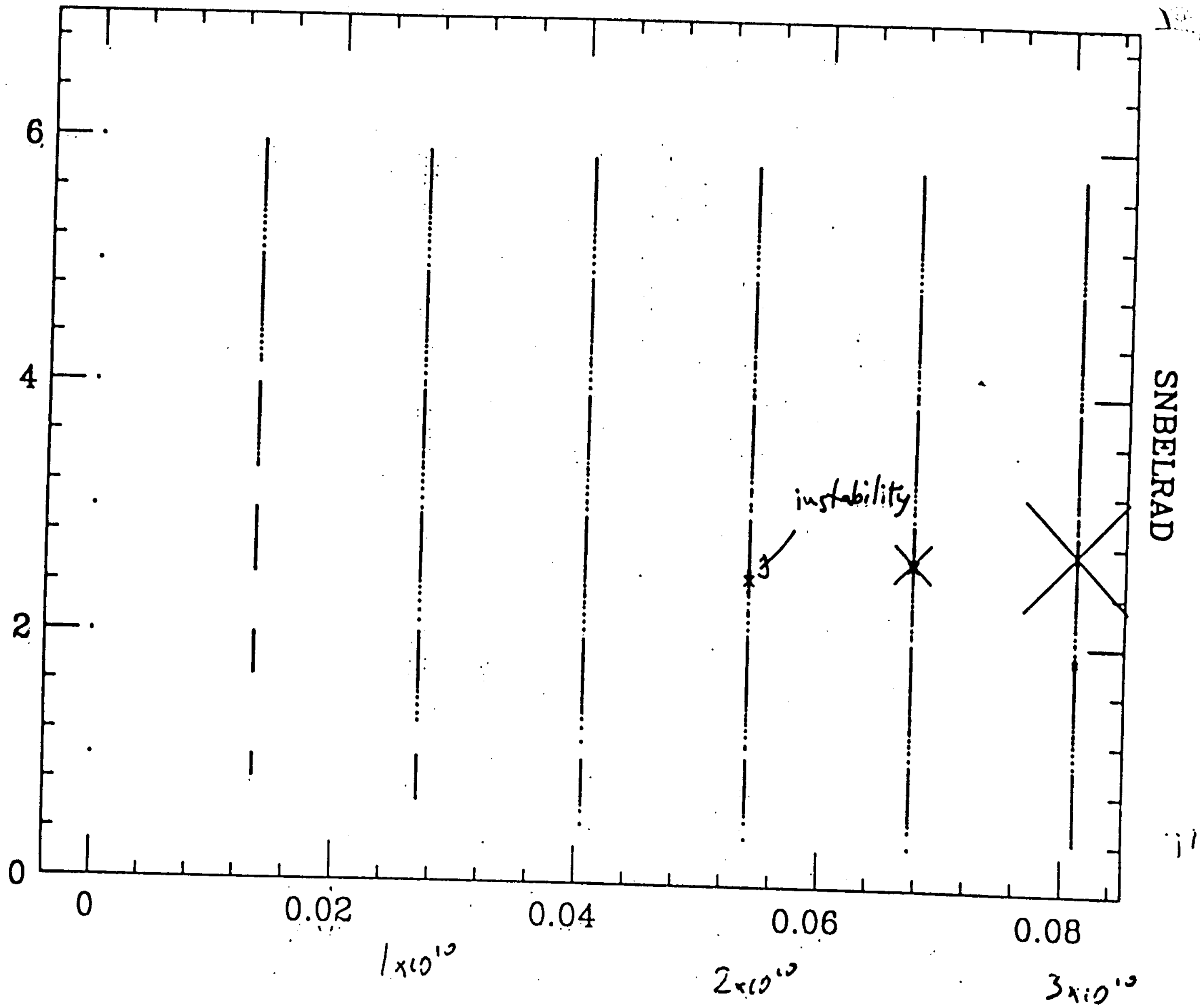

Summary for Old Machine

[Old, old → old] shielding bellows: N_{th} − $1.5\times10^{10} \rightarrow 3.0\times10^{10}$

Old: − σ_z, σ_δ vs N: good agreement between calculation + measurement

$\langle z \rangle$

	Meas.	Calc.
N_{th}	3×10^{10}	1.5×10^{10}
$(\nu_s)_{th}/\nu_{s0}$	2.6	2.5
$\frac{\Delta\nu_s}{\nu_{s0}}\left(\frac{10^{10}}{N}\right)$	+0.25	+0.27

− saw tooth

− not reliably seen in simulations

− could not run SLC above threshold

New Vacuum Chamber - to shorten bunch length, increase threshold

Measurement: Bunch Lengthening in Old vs New Vacuum Chamber

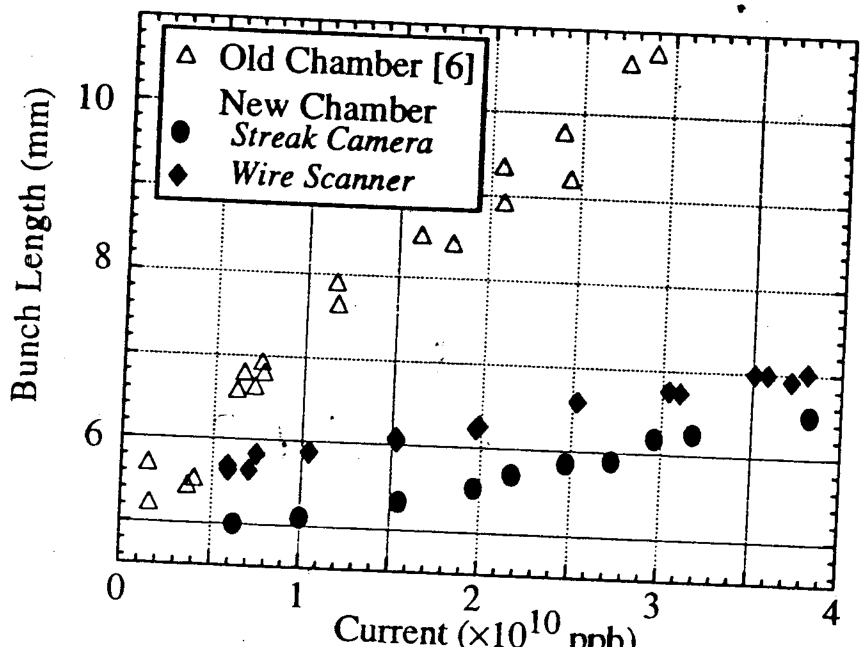

K. Bane, et al, 1995 PAC

Figure 2: Bunch length dependence on current. Bunch lengths are FWHM/2.35. $V_{RF} = 800$ kV.

- Shielding bellows: $N_{th} \to 1.5\times10^{10} \to 3.0\times10^{10}$
- In 1994 new, low impedance vacuum chambers were installed
  - bunch lengthening reduced
  - threshold went down from $3\times10^{10} \to 1.5\text{-}2.0\times10^{10}$
  - coherent frequency just below $2\nu_{s0}$
  - less severe: ran routinely above threshold $\sim 4.5\times10^{10}$; old machine could not run above threshold

The Bend-to-Quad Transitions

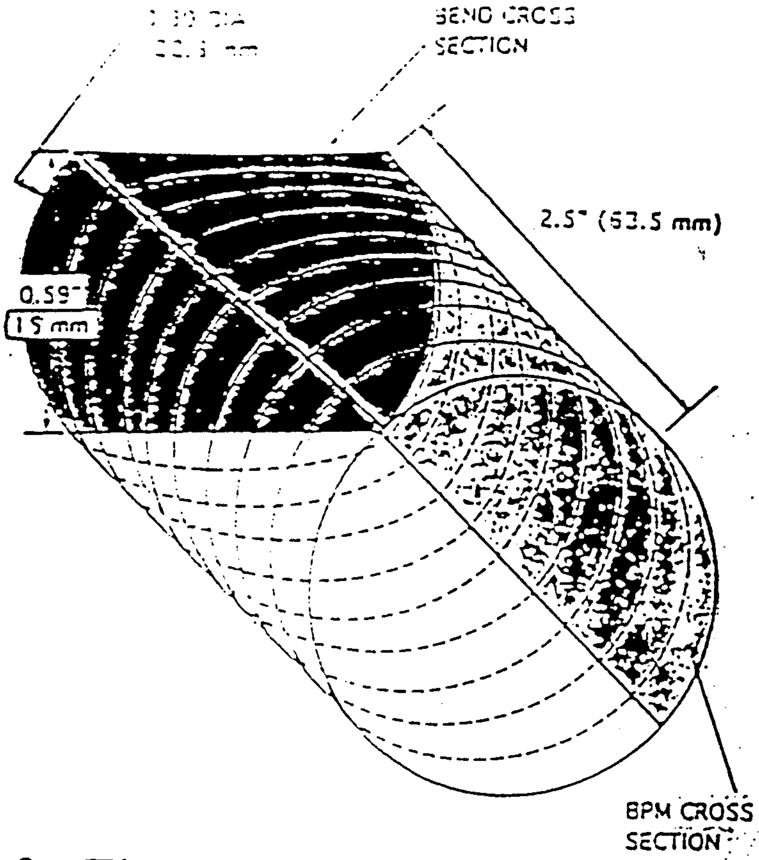

Fig. 3. The new bend-to-quad transition.

New bend-to-quad transitions

Weak Instability

see also Chao, Chen, Oide, 1995 PAC

K. Oide has shown that a purely resistive machine is unstable, that it has a (weak) growth rate varying as $\sim e^{aN^2t}$, and that it can be stabilized by a small amount of inductance (Landau damping)

Whereas the normal (strong) instability is often characterized by two azimuthal modes coupling, this instability can be characterized by two radial modes, with the same azimuthal mode number, coupling

Note: Boussard criterion does not apply to the weak instability

- See Chao, et al double waterbag model. Asymmetry of mode is important.
- That such a mode can exist was never appreciated before

K. Bane, K. Oide, 1995 PAC

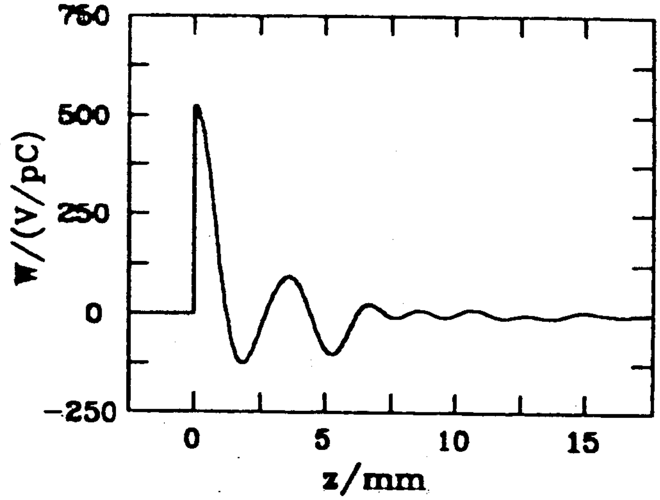

Green Function for New Chamber

Fig. 1. The wakefield used for the simulations.

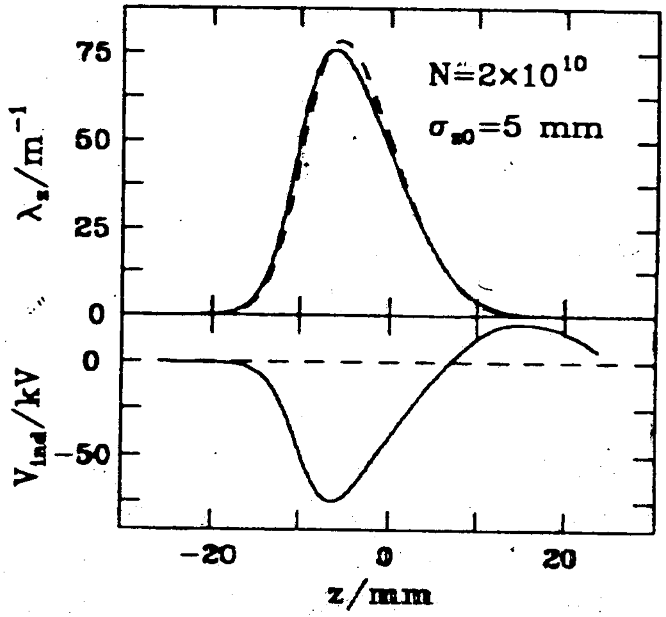

Haissinski solution

Note: now have resistive machine

Fig. 2. A potential well example.

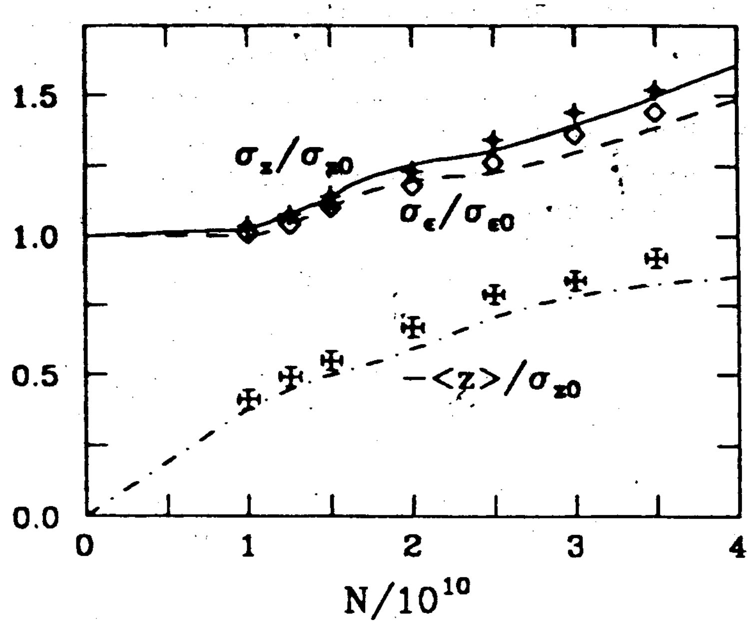

Simulation results comparing tracking (symbols) and the Vlasov solution (curves)

Fig. 5. Average bunch properties *vs* N. Shown are tracking results (plotting symbols) and the

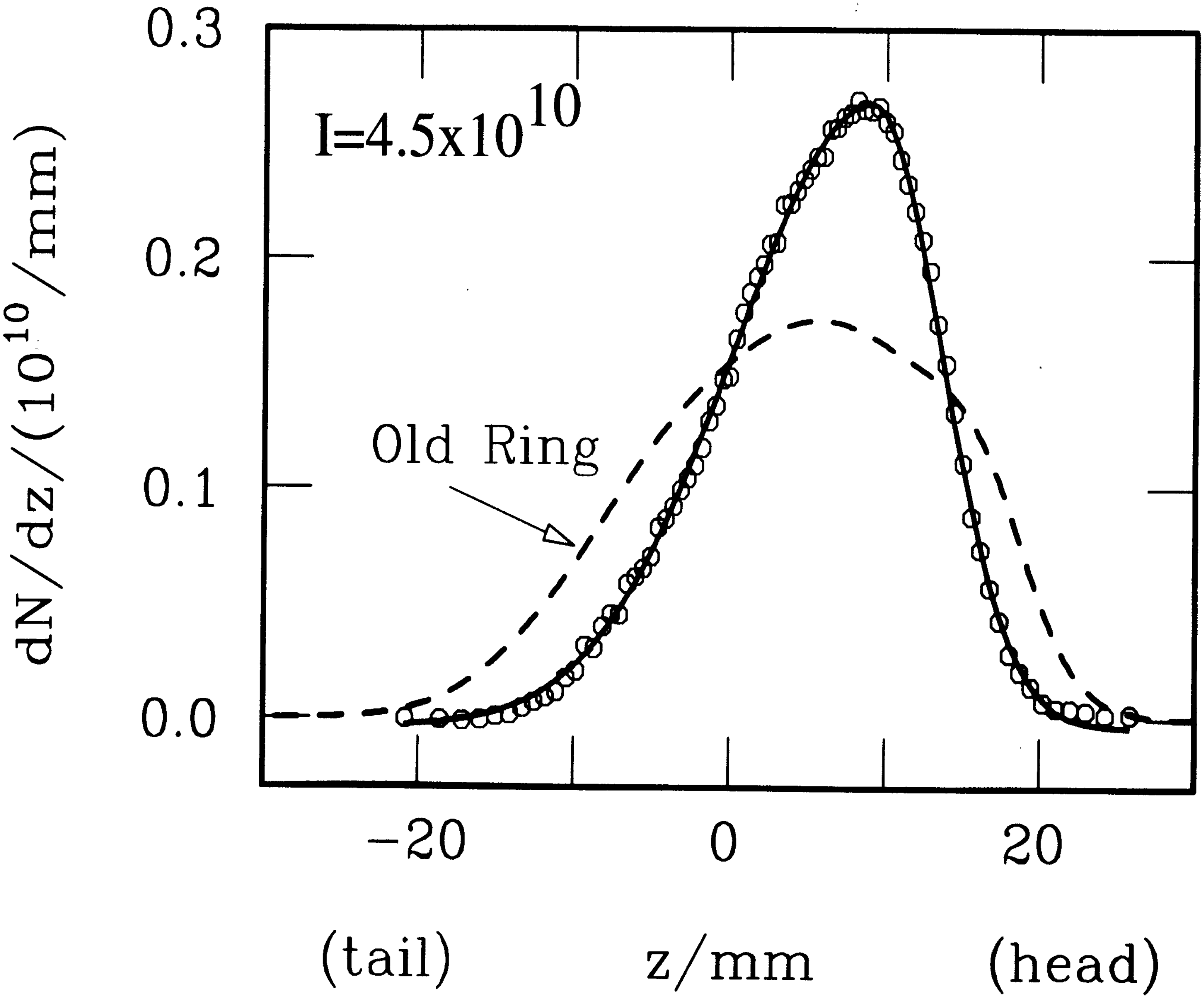

0.3
0.2
0.1
0.0
dN/dz/(10^{10}/mm)
I=4.5x10^{10}
Old Ring
−20
0
20
(tail)
z/mm
(head)

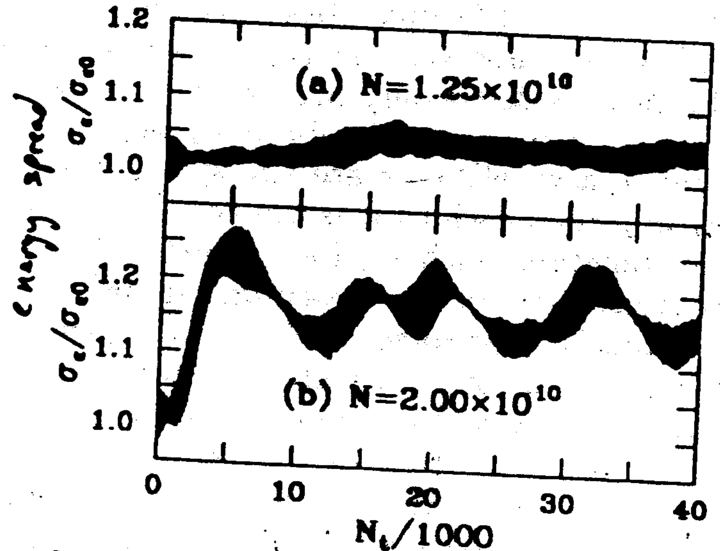

Fig. 3. The turn-by-turn rms energy spread just above threshold (a) and at a higher current. (b)

Examples of tracking showing fluctuations above threshold

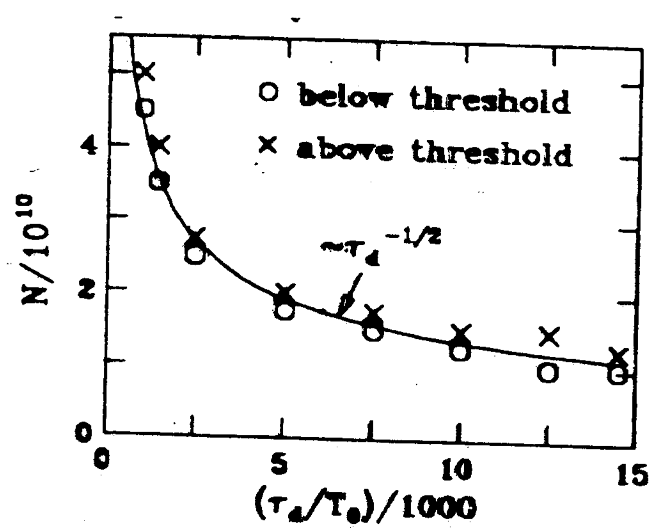

Fig. 4. N_{th} *vs.* τ_d obtained by tracking.

threshold as a function of damping time used in tracking program

$\Rightarrow$ growth $\sim e^{aN^2t}$

mode of instability

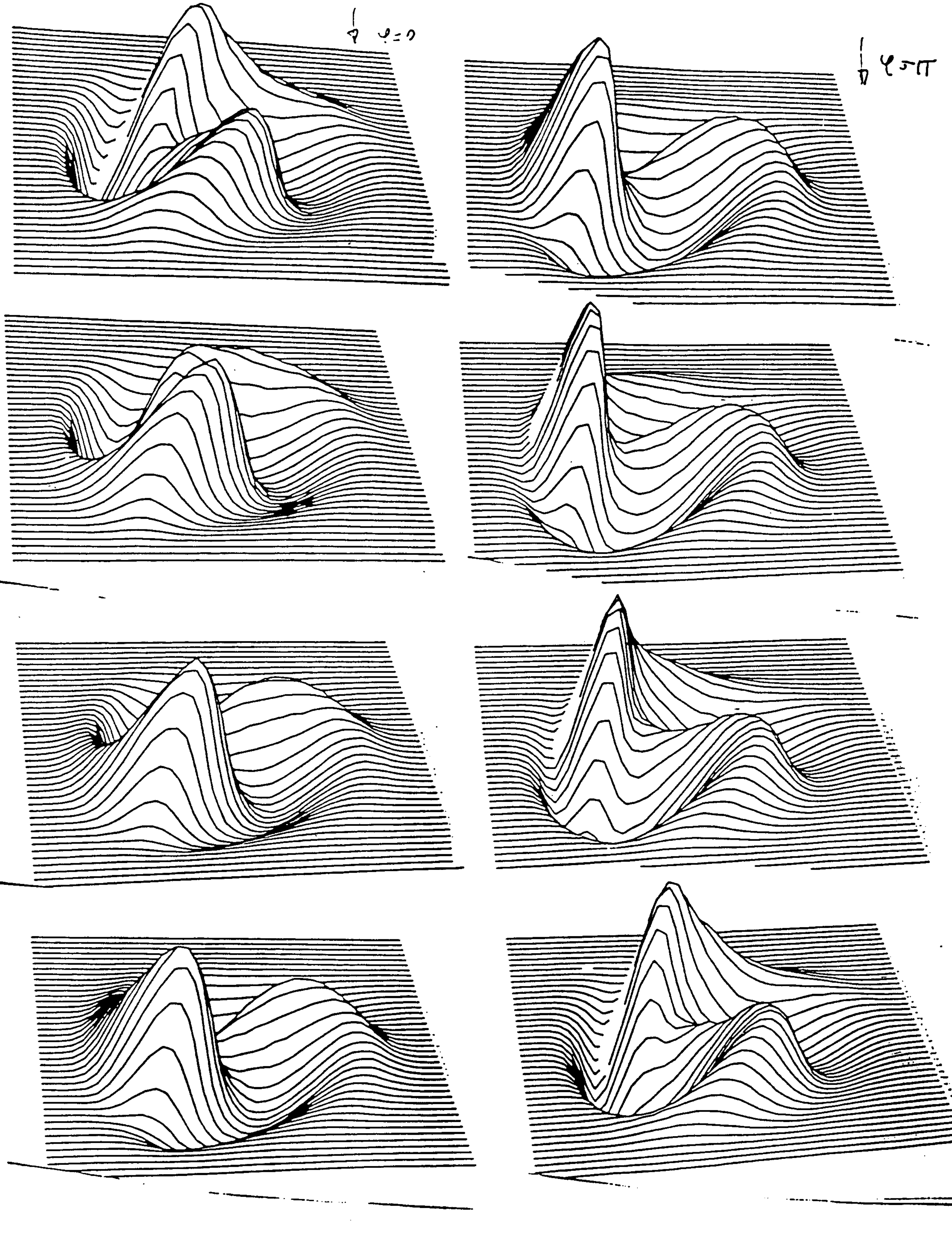

$N = 4.5 \times 10^{10}$, New Ring, Simulation

Tracking

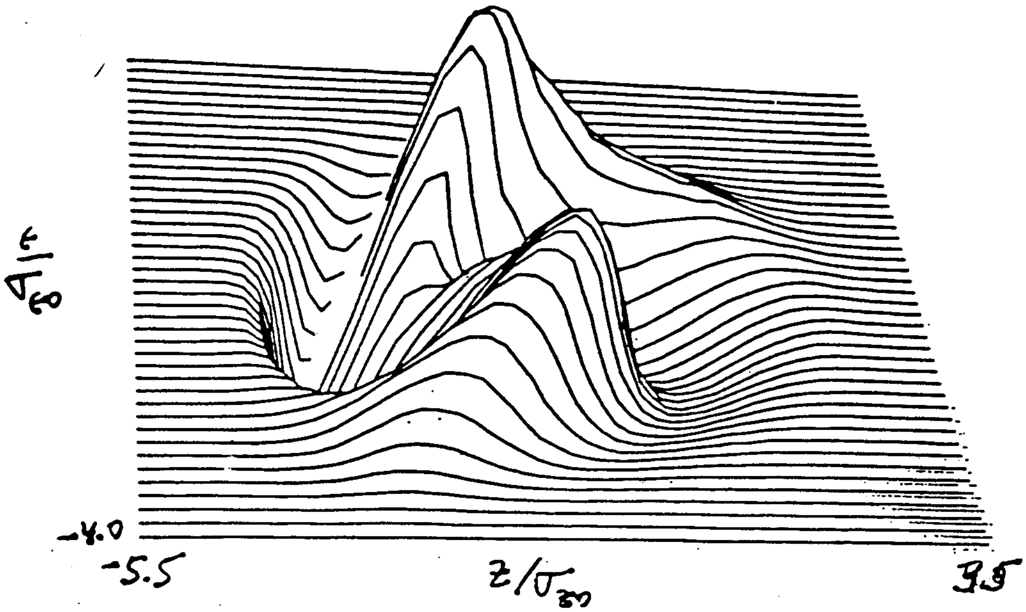

(b)

View

direction of wave motion

(b)

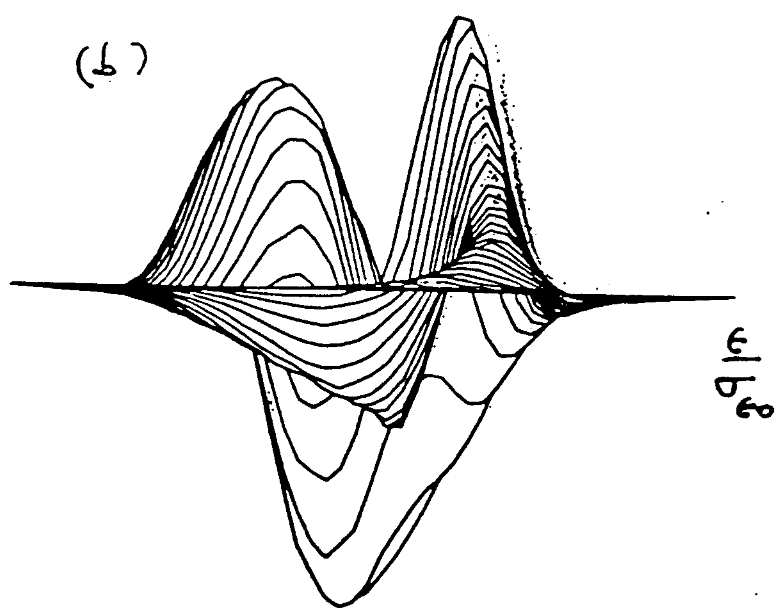

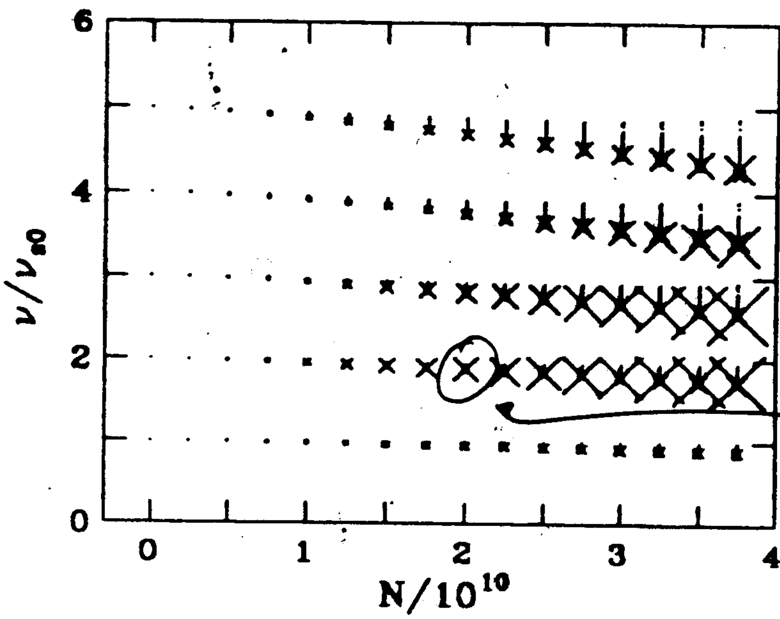

Modes of Vlasov solution (X's show unstable modes)

2 modes couple here

Fig. 7. Modes obtained by the Vlasov method.

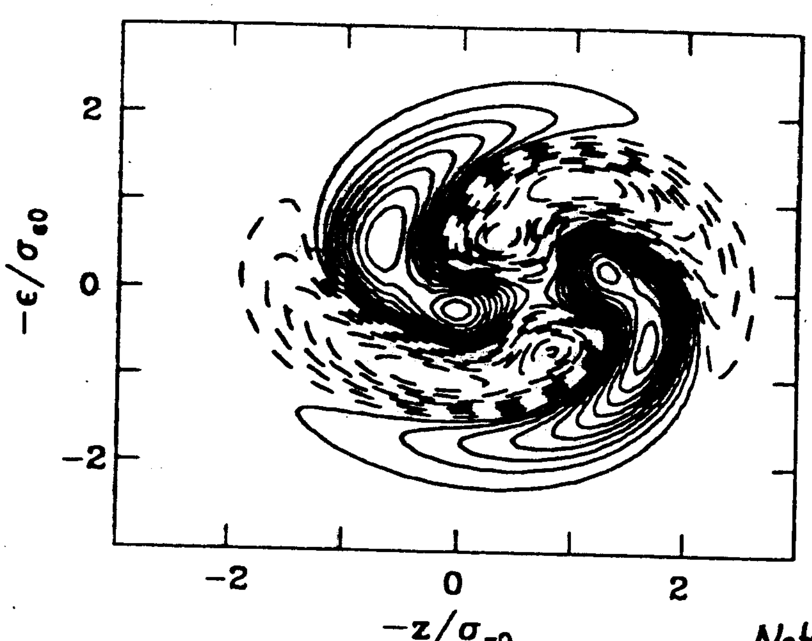

Shape of first unstable mode with growth time < radiation damping time

Fig. 6. Mode shape at $N = 2 \times 10^{10}$.

Note: quadrupole in nature

Measurements of Sawtooth Behavior in New Chamber

- B. Podobedov — B. Podobedov, R. Siemann, 1997 PAC.

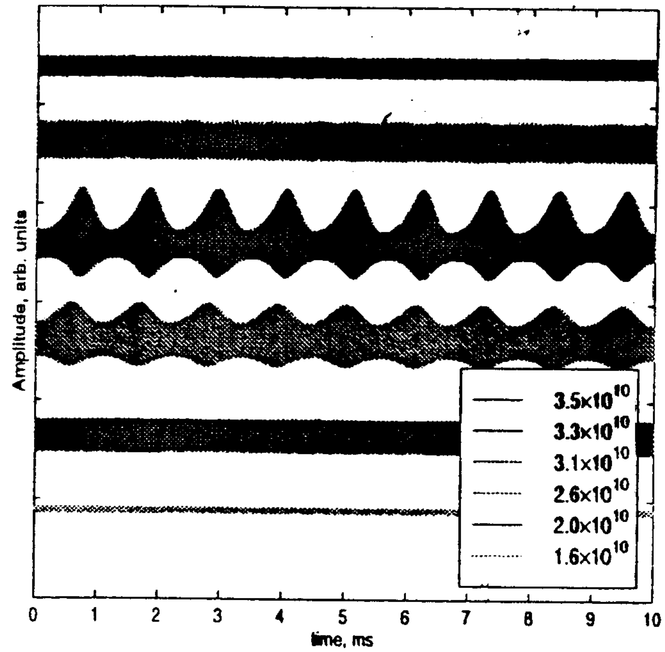

Figure 4. Oscilloscope traces of the instability signal for different values of stored charge.

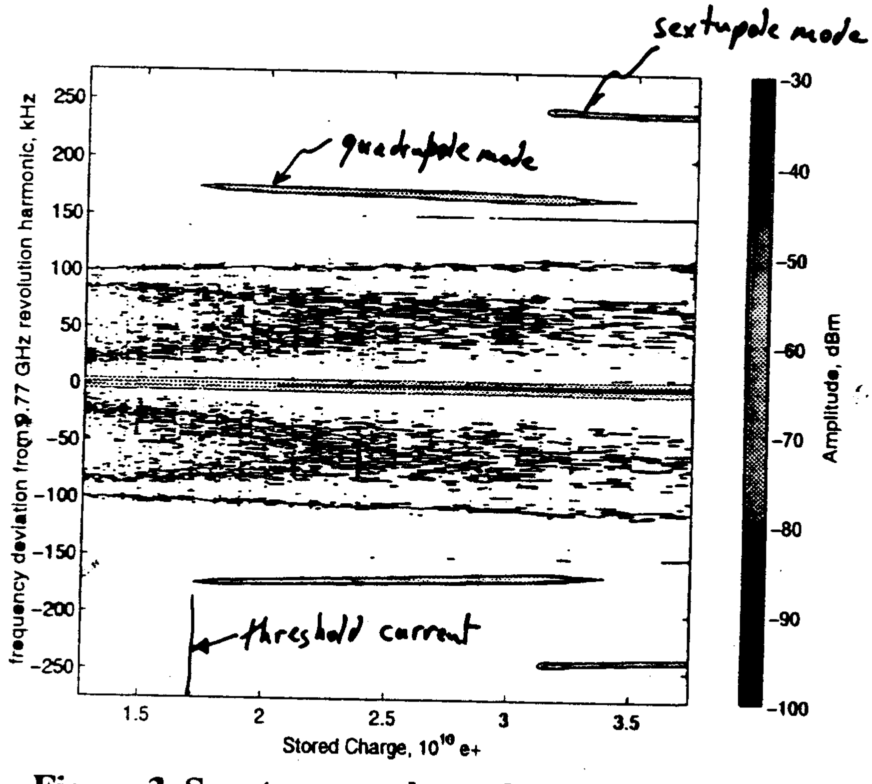

Figure 3. Spectrum analyzer data vs. stored charge.

Summary for Current Machine

- simulation: threshold (results) very sensitive to small amount of pure inductance [Landau damping]

$$\Delta(Z/n) = i\,0.1\,\Omega \Rightarrow \Delta N_{th} = 1\times10^{10}$$

- if $i0.1\Omega$ added, good agreement with measurement $\overline{\sigma_z}, \overline{\sigma_\epsilon}$, though large fluctuations in simulations for $N > N_{th}$

	Meas.	Calc.
N_{th}	$1.5-2.0\times10^{10}$	2.0×10^{10}
$(\nu_s)_{th}/\nu_{s0}$	1.77	1.87
$\frac{\Delta\nu_s}{\nu_{s0}}\left(\frac{10^{10}}{N}\right)$	-0.06	-0.07

- Saw tooth [few percent of beam performs transient behavior]
  - not as serious as before: routinely operated above threshold (4.5×10^{10})
  - not reliably simulated

How can we understand that when impedance was reduced N_{th} dropped?

Old machine:

inductive => large tune spread => weak instabilities are Landau damped

strong instability at 3×10^{10}

New machine:

resistive => little tune spread → we see a weak instability at

$1.5 - 2.0 \times 10^{10}$

strong instability has not been seen

[> 5×10^{10} according to calculation]

Why was weak instability not predicted?

Old/New Machine

- average of $\mathrm{Re}\,Z$, $\mathrm{Im}\,Z$ over bunch spectrum accurate

- unstable mode characteristics, eg $\frac{\Delta\nu}{\Delta I}$ agree pretty well

- Threshold ?

- Sawtooth ?

To avoid weak instability in NLC

- higher harmonic cavity - passive ok

- adjustable inductance (?) - preferably slots, holes in cavity walls

only a little tune spread is needed